

Simultaneously improving the tensile strength and ductility of the AlN_p/Al composites by the particle's hierarchical structure with bimodal distribution and nano-network



Fenghua Lu^a, Jinfeng Nie^{a,*}, Xia Ma^b, Yusheng Li^a, Zhouwen Jiang^c, Yong Zhang^c, Yonghao Zhao^a, Xiangfa Liu^{b,**}

^a Nano and Heterogeneous Materials Center, School of Materials Science and Engineering, Nanjing University of Science and Technology, Nanjing, 210094, China

^b Key Laboratory for Liquid-Solid Structural Evolution and Processing of Materials, Ministry of Education, Shandong University, Jinan, 250061, China

^c Herbert Gleiter Institute of Nanoscience, School of Materials Science and Engineering, Nanjing University of Science and Technology, Nanjing, 210094, China

ARTICLE INFO

Keywords:

Al composites
Hierarchical structure
AlN_p network
Strength
Ductility

ABSTRACT

Generally, metal matrix composites with homogenous microstructure exhibit good performance in mechanical properties, however, the shortcomings of limited strengthening effect by homogenous distributed reinforcements have been shown up in recent studies. In this work, the effect of reinforcement particles' hierarchical structure with bimodal distribution and nano-network on tensile properties of the AlN_p/Al composites has been studied. A novel AlN_p/Al composite with hierarchical structure has been fabricated using the in-situ liquid-solid reaction and hot extrusion, in order to further improve the mechanical properties. Furthermore, the AlN_p/Al composite was processed by rotary swaging (RS) to obtain a more uniform structure. The results show that the AlN_p/Al composites with hierarchical microstructure exhibit a superior ultimate tensile strength of ~410 MPa with uniform elongation of ~9.7%. However, the ultimate tensile strength and ductility of the AlN_p/Al composite after swaging treatment decrease to 370 MPa and 6.7%, respectively. It can be concluded that the hierarchical structure has a distinct superiority in simultaneously improving the strength and ductility of the Al based composite over the homogenous structure. Furthermore, the strengthening and toughening mechanisms have been discussed as well.

1. Introduction

Most engineering composites, including polymer matrix composites and metal matrix composites (MMCs), have been always controlled to obtain a uniform distribution of reinforcement in matrix on the basis of traditional engineering alloys [1–3]. Generally, it is considered that the composites with a homogeneous microstructure show a definite improvement in partial properties compared to the matrix [4]. However, many investigations carried out by tailoring the composite microstructure of discontinuously reinforced aluminum matrix composites (DRAMCs) indicates that the reinforcements can only play a limited role in uniform microstructure and the mechanical properties can be further improved by modifying the architecture [5,6]. A possible route to enhancing the strength/toughness ratios of composites is by assembling metals with other components to form novel reinforcements or

hierarchical structures [7].

Al-based MMCs (Al-MMCs) is often utilized in aerospace systems and automotive industries because of its light weight, excellent resistance to corrosion, good thermal and nonmagnetic properties [8–10]. Al-MMCs fabricated by in situ methods are popular due to their excellent properties and low cost [11,12]. In the previous work [13], a novel Al-based composite exhibiting the superior mechanical properties has been specially designed by in-situ assembling AlN_p network in the Al matrix. The novel particles' network can strengthen Al matrix effectively like the skeleton to human body. In order to verify the superiority of AlN_p network directly, a more homogeneous microstructure is supposed to be achieved as a suitable referencing object. However, the high strength particle network formed accompanied by in-situ liquid-solid reaction, the following heat treatment and low plastic deformation have little effect on the variation of the architecture.

* Corresponding author.

** Corresponding author.

E-mail addresses: niejinfeng@njust.edu.cn (J. Nie), xfliu@sdu.edu.cn (X. Liu).

In order to obtain a more homogeneous microstructure, the rotary swaging (RS) as a severely plastic deformation (SPD) processing is employed to the AlN_p/Al composite in this work. The main purpose is to revealing the superiority of hierarchical structure involving AlN_p network in strengthening and toughening the Al composites through the comparison with the homogeneous microstructure.

2. Experimental

2.1. Fabrication of AlN_p/Al composites with network and homogeneous microstructure

A novel Al based composite with network-structured AlN_p was fabricated using the in-situ liquid-solid reaction and hot extrusion as reported in our previous work [13], which is named as EXT sample. The mass fraction of AlN_p in the composites was 8.2 wt%. The size of initial material was $\sim 80 \pm 2$ nm in diameter, which was extruded at about 500°C with an extrusion ration of $\sim 33:1$, and the obtained EXT sample was 13.8 mm in diameter. Furthermore, the EXT sample was subjected to RS treatment at room temperature with a feeding speed of \sim to a certain equivalent strain mm/s for 0.2 and 0.6 (named as RS0.2 and RS0.6), respectively. The equivalent strain, ε_{eq} , is calculated using the relationship [14]:

$$\varepsilon = 2 \ln \frac{D_0}{D} \quad (1a)$$

1where D_0 and D are the diameters of the sample before and after RS, respectively. Thereby, the particles' network-structure was supposed to be broken to some extent during RS processing and a more homogeneous microstructure was achieved.

2.2. Microstructural characterization and tensile test

The microstructure characteristic and fractography observation were performed by a scanning electron microscope (FESEM, Quanta 250F, worked at 15 kV) equipped with Oxford energy dispersive X-ray spectrometer (EDS) and transmission electron microscope (TEM TECNAI 20). The samples for microstructure observation were etched using 0.5 vol% HF after mechanical polishing in order to observe the AlN_p clearly. Thin foils for TEM observations were prepared with mechanical polishing to the thickness of 25 μm . The specimens were finally polished by ion beam using Gatan 691 precision ion polishing system (PIPS). The room temperature tensile tests were carried out using an Instron hydraulic frame universal testing machine at a constant crosshead speed of 0.9 mm/min. The specimens were 5 mm in gauge length and 2 mm in gauge width.

3. Results

3.1. Microstructure features

As shown in Fig. 1(a), the initial Al powder is spherical with the size of about 20 μm . After in-situ liquid-solid reaction, AlN particles are formed in the matrix along with the obvious rich and lean domains as shown in Fig. 1(b). Fig. 2 shows the SEM images of the three different AlN_p/Al composites on the cross section (perpendicular to the extrusion direction). The EDS point analysis of the AlN particles in the matrix is shown in Fig. 2(b). The inhomogeneous distribution of AlN_p can be observed and the AlN particle-rich and particle-lean domains constitute a bimodal structure, indicating that a hierarchical microstructure is formed in the EXT sample. In order to achieve a homogeneous microstructure to compare with the hierarchical counterpart, the EXT samples were subjected to RS deformation processing with different equivalent strains for 0.2 and 0.6, respectively. The distribution of AlN_p after RS deformation is also shown in Fig. 2(c) and (d). It can be seen that the original distribution of AlN_p has changed significantly during the RS deformation treatment and the observed particle-lean area becomes smaller.

For a more comprehensive observation, the characteristic of composites on longitudinal section (parallel to the extrusion direction) are exhibited in Fig. 3. The inhomogeneous distribution of AlN_p is also observed on longitudinal section similar to that on transversal section. Meanwhile, it is worthy to note that most of the AlN_p are connected with each other from nano-scale to the micro-scale, which constructs a network structure at a higher magnification as shown in Fig. 3(b), which was also proved in our previous work [13]. In the bimodal structure, the fraction of particle-lean domains is estimated to be about $39.2\% \pm 3\%$ (Fig. 3(a)). After deformation, it can be seen that the bimodal structure has been changed to some extent as displayed in Fig. 3(c) and the original continuous AlN_p networks have been broken significantly (Fig. 3(d)). The fraction of particle-lean domains is estimated to be decreased to about $16.5\% \pm 2\%$ (Fig. 3(c)). With the further increase of the deformation strain up to 0.6, the bimodal structure can hardly be observed. The fraction of particle-lean domains is estimated to be smaller than $7.8\% \pm 1.5\%$ (Fig. 3(e)). Meanwhile, the AlN particles are dispersed similar to sample RS0.2 at a smaller scale (Fig. 3(e) and (f)). Furthermore, the rough statistics of particle size inset in Fig. 3(b, d and f). It can be seen that the mean size of AlN_p decreases from 92 nm to 85 nm, 80 nm with the increasing deformation.

Moreover, TEM has been further used to characterize the change of bimodal structure at a higher magnification. Fig. 4a and b shows the TEM micrographs of sample EXT, in which particle-lean domains and the particle rich strips can be observed clearly as indicated by the arrows. The coarse α -Al grains are elongated in particle-lean areas. Meanwhile, the α -Al grains in particle-rich domains are refined drastically to ultrafine grains due to the pinning effects of AlN_p on the dislocations during the extrusion process (Fig. 4(b)). The mean grain size of α -Al matrix in EXT sample has been calculated to about 1.34 μm . The microstructure change after RS treatment is shown in Fig. 4(c and d) and

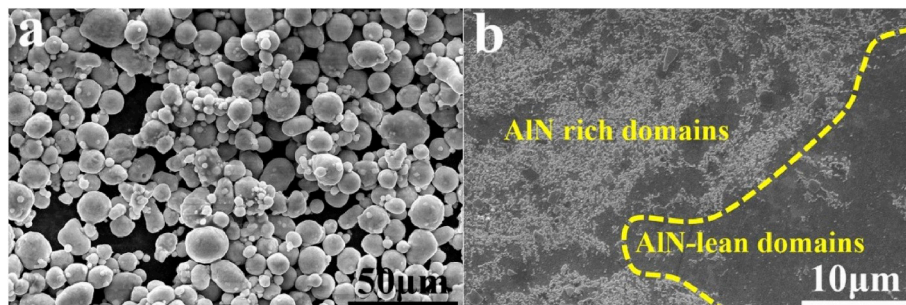


Fig. 1. SEM micrographs showing the microstructure of Al powders (a) and the as sintered AlN_p/Al composites before extrusion (b).

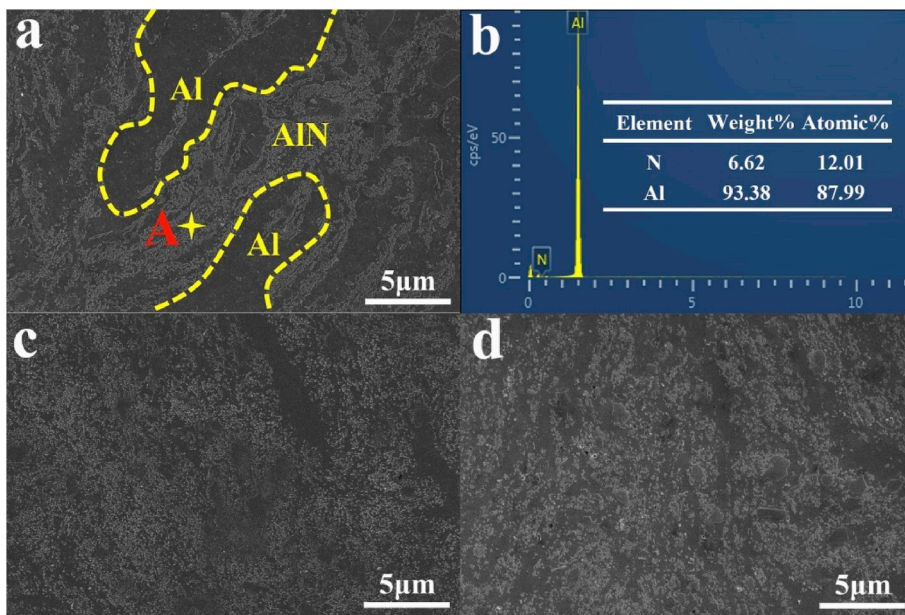


Fig. 2. SEM showing the distribution of AlN particles on cross section: (a) sample EXT; (b) EDS results of point A (a); (c) sample RS0.2; (d) sample RS0.6.

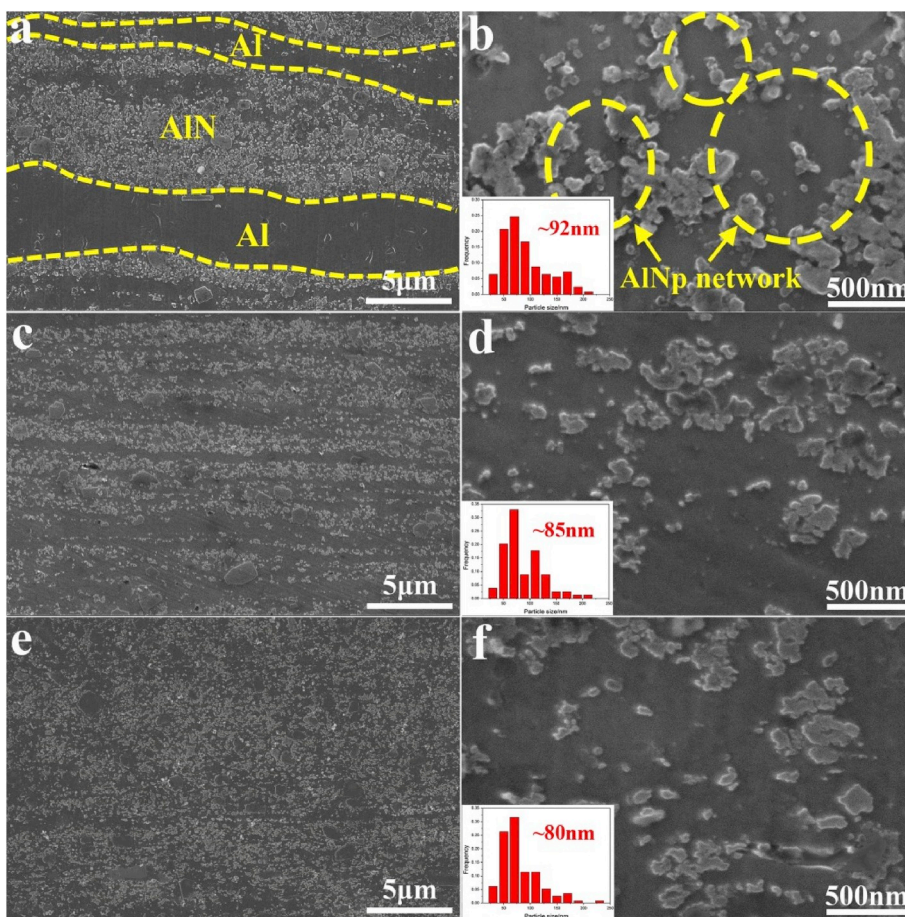


Fig. 3. AlN_p distribution of different samples on longitudinal section: (a, b) sample EXT; (c, d) sample RS0.2; (e, f) sample RS0.6.

the obvious bimodal structures cannot be seen clearly, which is the same as verified by SEM. Most of the original elongated coarse-grains have been refined further and a more homogeneous microstructure has formed in the composites. The mean grain size of α -Al matrix has been

reduced to about 0.94 μm and 0.84 μm , respectively, and an ultrafine grained microstructure with has been obtained.

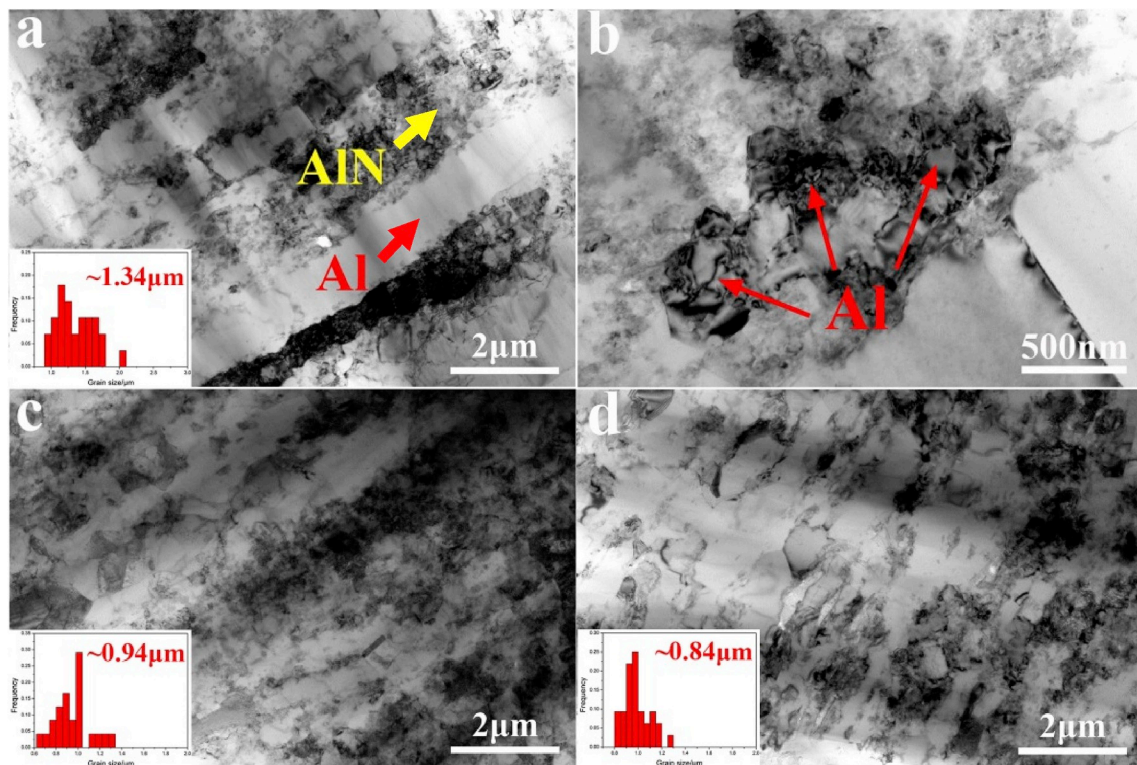


Fig. 4. TEM images of different AlN_p/Al composites showing the morphology and distribution of AlN particles and α-Al grains: (a, b) sample EXT; (c) sample RS0.2; (d) RS0.6.

3.2. Tensile properties of the AlN_p/Al composites

To compare the room temperature tensile properties of AlN_p/Al composite containing hierarchical structure with that having a more homogeneous microstructure, Fig. 5 exhibits the engineering stress-strain curves of different composites and the detail is given in Table 1. The yield strength (YS) of the EXT sample is ~350 MPa and the ultimate tensile strength (UTS) is ~410 MPa, with the corresponding uniform elongation (UE) and elongation to failure (EI) of 9.7% and 12.7%, respectively. It is worthy to note that YS of the samples has been hardly changed after the RS treatment, although the grains are refined and more uniform microstructure has been obtained. While, the UTS of the composites decreased from 410 MPa to 392 MPa and 370 MPa,

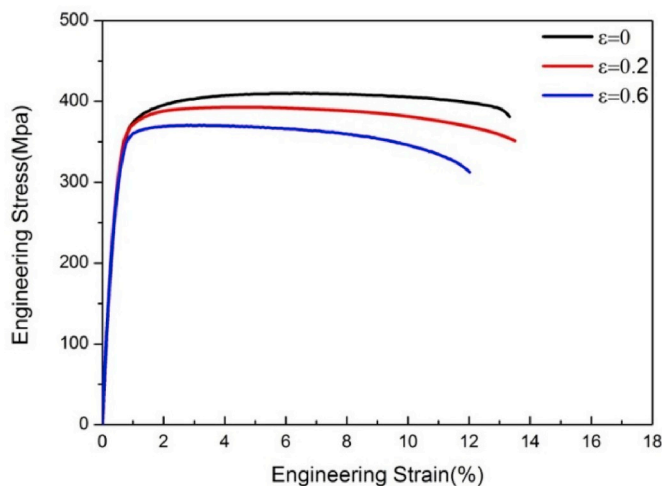


Fig. 5. Engineering tensile stress-strain curves of composites with different microstructures.

Table 1

Mechanical property of the three AlN_p/Al composites at RT.

Samples	YS/MPa	UTS/MPa	UE/%	EI/%
EXT	350	410	9.7	12.7
RS0.2	350	392	7.8	12.9
RS0.6	350	370	6.7	11.5

respectively. In addition to the reduced UTS value, it is surprised that the ductility of the RS treated samples has decreased to 7.8% and 6.7%, respectively. Therefore, it can be concluded that the AlN_p/Al composites with the hierarchical microstructure as the EXT sample behave an excellent comprehensive mechanical properties compared with that with a more uniform microstructure as the RS sample. That is to say that the hierarchical structure can simultaneously improve the strength and ductility for the AlN_p/Al composites.

4. Discussion

In order to reveal the strengthening and toughening mechanism of the composites with hierarchical structure, several main aspects have been discussed as follows:

The strength of composite, σ_c , can be evaluated by summing the strength of unreinforced matrix, σ_m , and the contributions relates to reinforcement strengthening effects, σ_p , therefore:

$$\sigma_c = \sigma_m + \sigma_p \tag{1b}$$

It has been known that Hall-Petch relationship can be used to describe the change of strength brought by the reduction of grain size [15,16]:

$$\sigma_y = \sigma_0 + \frac{K}{\sqrt{d}} \tag{2}$$

where σ_y is the yield strength, σ_0 is the initial strength, K is a constant

and d is the mean grain size. It can be seen from the statistical graph inset in Fig. 4 that the average grain size of Al grains decreases from $\sim 1.34 \mu\text{m}$ to $0.94 \mu\text{m}$, $0.84 \mu\text{m}$, respectively. Due to the grain refinement and the increased grain boundary strengthening, the yield strength of the composites is supposed to be increased.

However, from Table 1, the yield strength of different samples is almost the same ($\sim 350 \text{ MPa}$). Therefore, it can be concluded that the strengthening contribution from the AlN particle is reduced after RS treatment, which is induced by the broken of the particle network structure. That is to say, the network structure contributes significantly to the yield strength in the EXT sample.

As we all known, when the distribution of reinforcement particles in the matrix is inhomogeneous, different regions appear including reinforcement-rich regions and reinforcement-lean regions. According to the patterns of reinforcement-rich regions, there are four different kinds consist of A: isolated reinforcement-rich phase [17], B: Bar and laminated/ring-like microstructures [18], C: 3D continuous reinforcement-rich phase with isolated reinforcement-lean phase [19] and D: Bi-continuous reinforcement-rich phase and reinforcement-lean phase [20]. Generally speaking, the four patterns are distinguished into two categories from different scale. Pattern A, C and D are microstructurally inhomogeneous but macroscopically homogeneous, while Pattern B is adverse.

Based on the above analysis for the AlN_p/Al composites with hierarchical microstructure, it belongs to the typical bimodal distribution of AlN particles in micron scale. The particle-rich and particle-lean domains embed in a random homogenous effective medium to solve non-linear inclusion problems, so that the properties of bimodal composites can be determined [21]. Using the Eshelby theory as a starting point, the stress in different domains as a function of the applied stress σ_A can be expressed as:

$$\sigma_{rich} = \left(\frac{5C_{rich}}{2C_{rich} + 3C_{HEM}} \right) \sigma_A \quad (3)$$

$$\sigma_{lean} = \left(\frac{5C_{lean}}{2C_{lean} + 3C_{HEM}} \right) \sigma_A \quad (4)$$

where C_{rich} , C_{lean} and C_{HEM} are the effective moduli of rich domains, lean domains and the homogenous effective medium. The self-consistent theory is used to connect the stresses in the particles and matrix to the composites:

$$f\sigma_{rich} + (1-f)\sigma_{lean} = \sigma_A \quad (5a)$$

where f is the volume fraction of particle-rich domains.

Following the above analysis, K. T. Conlon and D. S. Wilkinson [21] show that the inhomogeneous particle distribution significantly

improves the strength compared with the homogeneous structure. However, their result just applies well to the compression test. When this type of materials is tested in tensile test [22], the stress–strain curve of the uniform and bimodal composites are similar. The main reason is that the load is transferred from particle-lean to the particle-rich areas and damage occurs in particle-rich domains during tensile test, therefore, the strength of composites drops due to the loss of load bearing capacity in particle-rich regions.

Different from K. T. Conlon and D. S. Wilkinson, our composites with hierarchical microstructure contain the AlN_p network in particle-rich regions at a smaller scale. The good bonding in AlN/Al interface and AlN_p network structure can effectively hinder the propagation of microcracks [23], thus the load capacity keeps high in particle-rich regions. Consequently, the hierarchical composites behave higher ultimate tensile strength than those with uniform microstructure.

In order to analyze the differences in the ultimate tensile strength, Fig. 6 compares the strain hardening behaviors between the composites with hierarchical and a more uniform microstructure. The truncation of true stress–strain curves and strain hardening rate curves relies on Considère criterion [24]:

$$\left(\frac{\partial \sigma}{\partial \varepsilon} \right)_{\varepsilon} = \sigma \quad (5b)$$

where σ is the true stress and ε is the true strain. Fig. 6(b) shows the normalized strain hardening rate:

$$\Theta = \frac{1}{\sigma} \left(\frac{\partial \sigma}{\partial \varepsilon} \right) \quad (6)$$

It can be seen that the Θ value of composite with hierarchical structure is always higher than those with a more uniform microstructure throughout the entire tensile deformation. The main reason for the lower Θ value of the RS sample is supposed to be that the original Al matrix grains have been refined further in the RS deformation process. It is known that the storage capacity of the dislocations for the smaller ultra-fine grains has been reduced due to the limited space in refined grains, which hinders the dislocations inner grains to mediate the plastic deformation [25]. While the coarse grains in the EXT samples can accumulated more dislocations, and thus a higher strain hardening rate can be achieved. Therefore, the UTS of hierarchical composites ($\sim 410 \text{ MPa}$) are higher than those with homogenous structure in this work.

According to the variation of different samples' elongation, the toughening mechanism involving the Al matrix and reinforcement distribution are discussed. In view of the strain hardening abilities of the different composites, the reduction of work hardening capacity in matrix not only affects the UTS of composites, but also influences the uniform elongation. It is known that the low strain hardening rate accelerates the

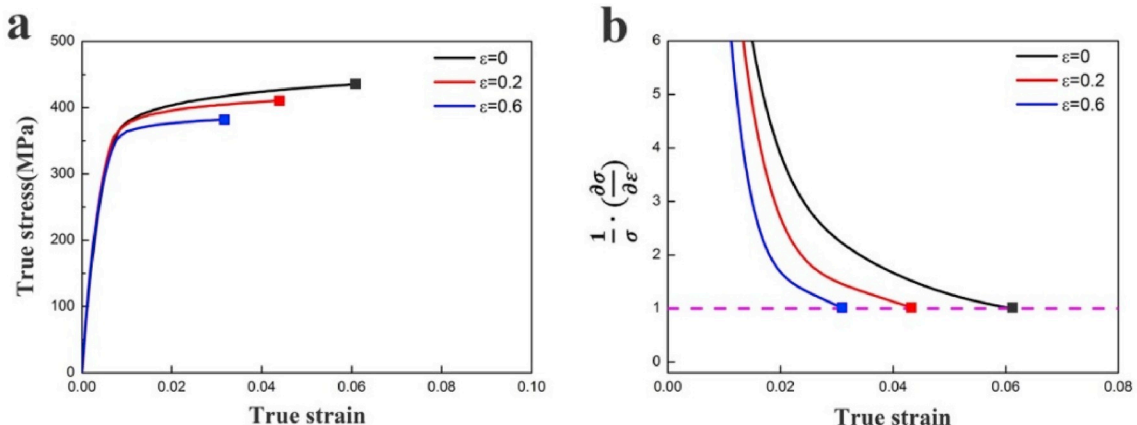


Fig. 6. (a) True stress–strain curves of the different composites; (b) the corresponding strain hardening rate curves of the three samples.

occurrence of plastic instability, and the localized deformation occurred in advance shortens the uniform strain [26,27]. Therefore, the uniform elongation is improved due to the increased strain hardening rate for the AlN_p/Al composites with hierarchical structure. From the viewpoint of different microstructure, it is known that the homogenous distribution of particles is helpful to inhibiting the strain localization during the tensile deformation [28,29] and contributes to the ductility enhancement. Thus, the inhomogenous distribution of AlN particles in the EXT samples will deteriorate the ductility to some extent. The particle distribution change of AlN in the matrix during RS deformation is helpful to ductility enhancement. However, the ductility decrease induced by the ultra-fine grains of Al matrix surpasses the ductility enhancement contributed by the reinforcement particles, a lower ductility is obtained in the RS samples. While, the coarse elongated $\alpha\text{-Al}$ grains supply more space for the accumulation and sliding of dislocations, which is a crucial aspect for the improved ductility for the hierarchical structured composites. When the ductility enhancement contributed from the coarse Al grains surpasses the ductility decrease induced by the reinforcement particles, a better UE ($\sim 9.7\%$) is achieved in the EXT sample. In addition, with a view to the stage from UTS to fracture, the elongation at crack propagation period increases from 3% to 5.1%, 4.8%, indicating that the more uniform microstructure after RS deformation zigzags the crack propagation. Therefore, no significant decline appears in elongation with the decrease of uniform elongation. Based on the above analysis, it can be seen that a simultaneously improved strength and uniform elongation can be attained by the reinforcement particles' hierarchical structure.

At the same time, considering that rotary swaging is a cold working process, the working softening of samples after RS processing is possibly related to localized cracks caused by RS processing. Figs. 2 and 3 show

that no cracks can be observed, however, the area shown in SEM images is too small to be convincible. Therefore, the fracture surfaces of different tensile samples are further investigated and shown in Fig. 7. The whole fracture surfaces can be observed in Fig. 7(a, c, e) at a low magnification and no cracks have been found, which suggests that the defects such as microcracks are not introduced to the samples during processing. Furthermore, amounts of dimples are observed in Fig. 7(b, d, f) at a higher magnification, which indicate the ductile fracture mode corresponding to tensile stress-strain curves. Therefore, the defects (localized cracks) should not be the reason of working softening. As discussed as the above, the ultra-fine grains of Al matrix play the dominant role in the work softening of the RS samples.

5. Conclusions

To evaluate the strengthening and toughening potential of the AlN_p/Al composites, a hierarchical structure constituted by bimodal distribution of AlN_p and AlN_p network structure and a more uniform microstructure have been designed in the present work. Based on the tensile properties comparison, it shows that the hierarchical structure can simultaneously improve the tensile strength and ductility of the AlN_p/Al composites, and a better comprehensive mechanical property (~ 410 MPa of UTS and $\sim 9.7\%$ of uniform elongation) has been obtained. The strengthening mechanism is attributed to the higher load bearing efficiency of AlN particle-rich domains in the matrix and the higher strain hardening rate. Meanwhile, the coarse elongated $\alpha\text{-Al}$ grains in hierarchical structure contribute to the good ductility, which supply more space for the accumulation and sliding of dislocations to mediate the plastic deformation.

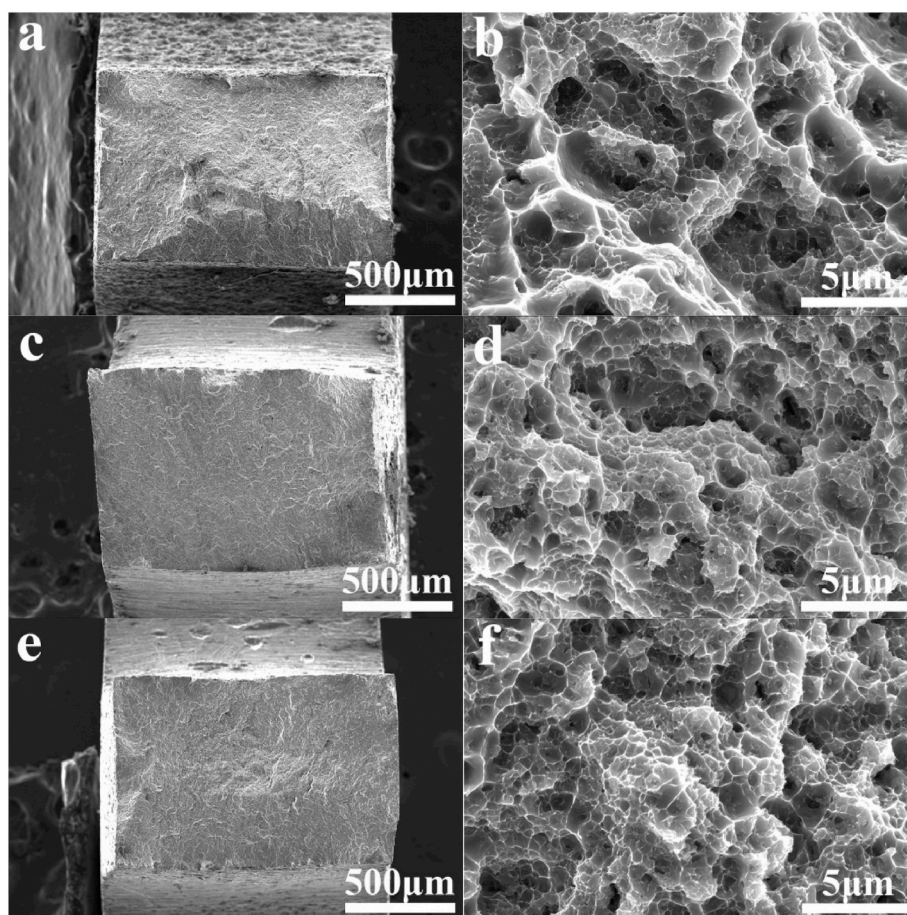


Fig. 7. The tensile fracture surfaces of different samples: (a, b) sample EXT; (c, d) sample RS0.2; (e, f) sample RS0.6.

Data availability

All data included in this study are available upon request by contact with the corresponding author.

Acknowledgements

This work was supported by grant from Key Program of National Natural Science Foundation of China (No. 51731007), the National Key R&D Program of China (No. 2017YFA0204403), National Natural Science Foundation of China (No. 51501092) and the Fundamental Research Funds for the Central Universities (No. 30919011405). The authors also want to acknowledge the support of the Jiangsu Key Laboratory of Advanced Micro-Nano Materials and Technology. SEM and TEM experiments are performed at the Materials Characterization and Research Center of Nanjing University of Science and Technology.

Appendix A. Supplementary data

Supplementary data to this article can be found online at <https://doi.org/10.1016/j.msea.2019.138519>.

References

- [1] Y.M. Youssef, R.J. Dashwood, P.D. Lee, Effect of clustering on particle pushing and solidification behaviour in TiB₂ reinforced aluminium PMMCs, *Composites, Part A* 36 (2005) 747–763.
- [2] S.C. Tjong, Y.W. Mai, Processing-structure-property aspects of particulate- and whisker-reinforced titanium matrix composites, *Compos. Sci. Technol.* 68 (2008) 583–601.
- [3] S.H. Kang, B.M. Jung, J.Y. Chang, Polymerization of an organogel formed by a hetero-bifunctional gelator in a monomeric solvent: preparation of nanofibers embedded in a polymer matrix, *Adv. Mater.* 19 (2007) 2780–2784.
- [4] J.F. Nie, F. Wang, Y.S. Li, Y.F. Liu, X.F. Liu, Y.H. Zhao, Microstructure and mechanical properties of Al-TiB₂/TiC in situ composites improved via hot rolling, *Trans. Nonferrous Metals Soc. China* 27 (2017) 2548–2554.
- [5] B. Kaveendran, G.S. Wang, L.J. Huang, L. Geng, Y. Luo, H.X. Peng, In situ (Al₃Zr_p+Al₂O_{3np})/2024Al metal matrix composite with controlled reinforcement architecture fabricated by reaction hot pressing, *Mater. Sci. Eng. A* 583 (2013) 89–95.
- [6] Z.Y. Hu, Z.H. Zhang, X.W. Cheng, Q. Song, S.P. Yin, H. Wang, F.C. Wang, Microstructure evolution and tensile properties of Ti-(Al_xTi_{1-x}) core-shell structured particles reinforced aluminum matrix composites after hot-rolling/heat-treatment, *Mater. Sci. Eng. A* 737 (2018) 90–93.
- [7] K. Lu, *Materials science. The future of metals*, *Science* 328 (2010) 319–320.
- [8] Z. Wang, R.T. Qu, S. Scudino, B.A. Sun, K.G. Prashanth, D.V. Louzguine-Luzgin, M. W. Chen, Z.F. Zhang, J. Eckert, Hybrid nanostructured aluminum alloy with super-high strength, *NPG Asia Mater.* 7 (2015) e229.
- [9] J.C. Williams, E.A. Starke, Progress in structural materials for aerospace systems, *Acta Mater.* 51 (2003) 5775–5799.
- [10] C. Borgonovo, D. Apelian, M.M. Makhlof, Aluminum nanocomposites for elevated temperature applications, *J. Occup. Med.* 63 (2011) 57–64.
- [11] H.B. Yang, T. Gao, H.N. Zhang, J.F. Nie, X.F. Liu, Enhanced age-hardening behavior in Al-Cu alloys induced by in-situ synthesized TiC nanoparticles, *J. Mater. Sci. Technol.* 35 (2019) 374–382.
- [12] D.S. Zhou, J. Tang, F. Qiu, J.G. Wang, Q.C. Jiang, Effects of nano-TiC_p on the microstructures and tensile properties of TiC_p/Al-Cu composites, *Mater. Char.* 94 (2014) 80–85.
- [13] X. Ma, Y.F. Zhao, W.J. Tian, Z. Qian, H.W. Chen, Y.Y. Wu, X.F. Liu, A novel Al matrix composite reinforced by nano-AlNp network, *Sci. Rep.* 6 (2016) 34919.
- [14] Y. Yang, J.F. Nie, Q.Z. Mao, Y.H. Zhao, Improving the combination of electrical conductivity and tensile strength of Al 1070 by rotary swaging deformation, *Results Phys.* 13 (2019) 102236.
- [15] E.O. Hall, The deformation and ageing of mild steel: II characteristics of the Lüders deformation, *Proc. Phys. Soc. Sect. B* 64 (1951) 742.
- [16] N.J. Petch, The cleavage strength of polycrystals, *J. Iron Steel Inst. London* 174 (1953) 25–28.
- [17] S. Kumai, J. Hu, Y. Higo, S. Nunomura, Effects of dendrite cell size and particle distribution on the near-threshold fatigue crack growth behaviour of cast Al-SiC_p composites, *Acta Mater.* 44 (1996) 2249–2257.
- [18] A.B. Pandey, B.S. Majumbar, D.B. Miracle, Laminated particulate-reinforced aluminum composites with improved toughness, *Acta Mater.* 49 (2001) 405–417.
- [19] H.B. Yang, T. Gao, G.L. Liu, X.J. Zhao, H.W. Chen, H.C. Wang, J.F. Nie, X.F. Liu, Simultaneously improving strength and ductility for Al-Cu-Mg alloy via threadiness array of TiC nanoparticles, *Materialia* 6 (2019) 100333.
- [20] S. Roy, J. Gibmeier, V. Kostov, K.A. Weidenmann, A. Nagel, A. Wanner, Internal load transfer in a metal matrix composite with a three-dimensional interpenetrating structure, *Acta Mater.* 59 (2011) 1424–1435.
- [21] K.T. Conlon, D.S. Wilkinson, Effect of particle distribution on deformation and damage of two-phase alloys, *Mater. Sci. Eng. A* 317 (2001) 108–114.
- [22] K.T. Conlon, E. Maire, D.S. Wilkinson, H. Henein, Processing and microstructural characterization of Al-Cu alloys produced from rapidly solidified powders, *Metall. Mater. Trans. A* 31 (2000) 249–260.
- [23] X. Ma, Y.F. Zhao, X.J. Zhao, T. Gao, H.W. Chen, X.F. Liu, Influence mechanisms of Cu or Fe on the microstructures and tensile properties at 350 °C of network AlNp reinforced Al composites, *J. Alloy. Comp.* 740 (2018) 452–460.
- [24] M.X. Yang, D.S. Yan, F.P. Yuan, P. Jiang, E. Ma, X.L. Wu, Dynamically reinforced heterogeneous grain structure prolongs ductility in a medium-entropy alloy with gigapascal yield strength, *Proc. Natl. Acad. Sci. U. S. A* 115 (2018) 7224–7229.
- [25] F. Dalla Torre, H. Van Swygenhoven, M. Victoria, Nanocrystalline electrodeposited Ni: microstructure and tensile properties, *Acta Mater.* 50 (2002) 3957–3970.
- [26] E. Ma, T. Zhu, Towards strength–ductility synergy through the design of heterogeneous nanostructures in metals, *Mater. Today* 20 (2017) 323–331.
- [27] Y.M. Wang, E. Ma, Strain hardening, strain rate sensitivity, and ductility of nanostructured metals, *Mater. Sci. Eng. A* 375–377 (2004) 46–52.
- [28] R.V. Kumar, R. Keshavamurthy, C.S. Perugu, P.G. Koppad, M. Alipour, Influence of hot rolling on microstructure and mechanical behaviour of Al6061-ZrB₂ in-situ metal matrix composites, *Mater. Sci. Eng. A* 738 (2018) 344–352.
- [29] R. Geng, F. Qiu, Q.L. Zhao, Y.Y. Gao, Q.C. Jiang, Effects of nanosized TiC_p on the microstructure evolution and tensile properties of an Al-Mg-Si alloy during cold rolling, *Mater. Sci. Eng. A* 743 (2019) 98–105.